



**Anomalous Floquet-Anderson insulator with quasiperiodic temporal noise**Peng-Peng Zheng <sup>\*</sup>, Christopher I. Timms, and Michael H. Kolodrubetz *Department of Physics, University of Texas at Dallas, Richardson, Texas, USA*

(Received 14 July 2022; revised 17 May 2023; accepted 23 August 2023; published 15 September 2023)

Time-periodic (Floquet) drive can give rise to novel symmetry breaking and topological phases of matter. Recently, we showed that a quintessential Floquet topological phase known as the anomalous Floquet-Anderson insulator is stable to noise on the timing of its Floquet drive. Here, we perturb the anomalous Floquet-Anderson insulator at a single incommensurate frequency, resulting in a quasiperiodic two-tone drive. Our numerics indicate that a robust topological phase survives at weak noise with topological pumping that is more stable than the case of white noise. Within the topological phase, we show that particles move subdiffusively, which is directly responsible for stabilizing topological transport. Surprisingly, we discover that when quasiperiodic noise is sufficiently strong to kill topology, the system appears to exhibit diffusive dynamics, suggesting that the correlated structure of the quasiperiodic noise becomes irrelevant.

DOI: [10.1103/PhysRevB.108.094207](https://doi.org/10.1103/PhysRevB.108.094207)

*Introduction.* Time-dependent Hamiltonians exhibit a wide variety of quantum phenomena that cannot be found in static systems [1]. For instance, periodic time-dependence, a.k.a. Floquet drive, opens up the possibility of discrete time crystals [2–9] and Floquet symmetry-protected topological states [10–29]. A canonical example of Floquet topology is the anomalous Floquet-Anderson insulator (AFAI), in which the insulating bulk has particles with nontrivial micromotion, even though they are stroboscopically localizable. Despite Anderson localization of the entire bulk, and thus a vanishing Chern number, the AFAI nevertheless has chiral edge states which remain robust to finite disorder.

More recently, we have shown that the AFAI remains stable in the presence of white noise, which breaks the time-periodicity of the Floquet problem. Not only is there a well-defined topological invariant in the presence of noise but also a quantized topological response—current pumped by the edge states—remains precisely quantized up to a timescale set by noise-induced diffusion [25]. While other papers have suggested formal definitions of topological invariants in open quantum systems via extensions of the Berry phase [30,31], our work suggests that Floquet systems provide unique robustness to noise due to the fact that topology is defined via time evolution of the entire manifold of states, rather than a gapped ground state.

Given that the ultimate loss of topological response is due to noise-induced diffusion, a natural question is what happens for systems between perfect periodic Floquet drive and white noise, in which such diffusive dynamics will be altered. Therefore, in this paper, we consider the important case of multifrequency drive, also known as quasiperiodic Floquet drive. Quasiperiodic drive is known to be interesting in a variety of systems, enabling novel topological phases of matter, symmetry breaking, and other extensions of Floquet theory [28,29,32–34]. Quasiperiodic drive has also been argued to

be consistent with many-body localization [35], which might enable these phases of matter to remain robust to infinite time even in the presence of interactions. Such drives are widely expected to modify the diffusive approach to equilibrium, but also, by extending the classification of Floquet topological phases, may enable true, infinitely long-lived topological states of matter.

In this paper, we consider the simplest case of replacing the white noise from the bath by a single incommensurate drive. We explore topological response in this bichromatically driven system and find finite-time quantization similar to the noisy case. Unlike the noisy case, quasiperiodic drive creates an unusual potential landscape in the frequency lattice, which changes diffusive transport into subdiffusive over a wide range of parameters. Subdiffusion extends the timescale of topologically quantized pumping, although it still eventually decays on timescales set by a power law of system size. In other models, one may be able to find regimes with localization in both spatial and frequency directions, for which the topological response would remain quantized to exponential time in system size. It might also be worth exploring the absolute diffusive regime that large chaos pushes the system into, but that will be beyond the scope of this paper.

*Model.* We begin with the conventional model of the AFAI, which consists of spinless fermions hopping on a two-dimensional square lattice. In the absence of noise or quasiperiodic drive, the Hamiltonian is given by a five step drive with period  $T$ , such that each step has period  $T/5$ . The first four steps involve hopping between select pairs of sites,

$$H_\ell = -J \sum_{\langle ij \rangle_\ell} c_i^\dagger c_j, \quad (1)$$

for  $\ell \in \{1, 2, 3, 4\}$  where the connected sites  $\langle ij \rangle_\ell$  are chosen such that the particles hop in a closed loop around the plaquette each Floquet cycle, as shown in Fig. 1. The hopping strength  $J$  is fine tuned to  $JT = 5\pi/2$  such that the particles hop exactly one site per step in the absence of noise or

<sup>\*</sup>pxz150930@utdallas.edu

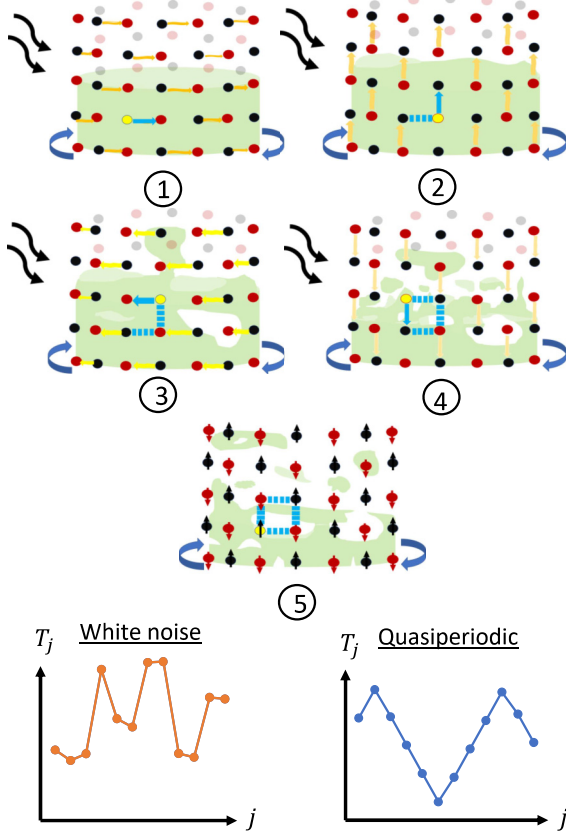


FIG. 1. Schematic representation of the five-step drive producing the quasiperiodically driven anomalous Floquet-Anderson insulator. In the absence of noise or disorder, bulk fermions hop around one plaquette during each cycle, returning to their original location (light blue arrows). Initially the bottom half of the cylinder is filled, but as time progresses, particles delocalize subdiffusively. Bottom panels illustrate white noise and triangular-wave quasiperiodic noise.

disorder. The final step is a staggered chemical potential,

$$H_5 = \Delta \sum_j \eta_j c_j^\dagger c_j, \quad (2)$$

where  $\eta_j = +1$  ( $-1$ ) on the  $A$  ( $B$ ) sublattice. We consider cylindrical geometry, with periodic boundary conditions in the  $x$  direction and open boundary conditions in the  $y$  direction. The system size is  $L \times L$  lattice sites. Finally, we add static chemical disorder,

$$H_{\text{dis}} = \sum_j \mu_j c_j^\dagger c_j, \quad (3)$$

to give Anderson localization. The strength of chemical potential disorder is set by  $W_x$  such that  $\mu_j$  is uniformly sampled between  $[-W_x, W_x]$ . Units are set by  $\hbar = 1$  and  $T = 2\pi$  throughout.

We add quasiperiodic noise to our model by varying the timings of the five steps. Instead of fixed period  $T/5$  per step, we use

$$T_j = \frac{T}{5}(1 + \delta_j), \quad (4)$$

where  $\delta_j \in [-W_t, W_t]$  is the temporal disorder of strength  $W_t$ . In this paper, we compare two types of noise: true temporal

disorder, i.e., white noise, in which the  $\delta_j$  are chosen independently and randomly as in Ref. [27], and quasiperiodic “disorder,” in which the  $\delta_j$  are a periodic function of time that is incommensurate with the original Floquet period  $T$ . In particular, we choose

$$\delta_j = W_t f\left(\frac{2\pi \Xi j}{5} + \Phi\right), \quad (5)$$

where  $f(\theta) = f(\theta + 2\pi)$  is a  $2\pi$ -periodic function,  $\Xi$  is an irrational number, which we choose as the golden ratio  $\Xi = (1 + \sqrt{5})/2$ , and  $\Phi$  is the initial phase of the drive. While a natural choice for  $f$  is a sinusoidal function, we instead choose the triangular wave:  $f(-\pi/2 < \theta < \pi/2) = \theta/(\pi/2)$ ,  $f(\pi/2 < \theta < 3\pi/2) = f(\pi - \theta)$ , such that the probability of a given  $\delta_j$  will be evenly distributed from  $-W_t$  to  $W_t$ , enabling direct comparison with white noise. For notational simplicity, since we wish to keep the Floquet period  $T$  constant, we instead think of this  $1 + \delta_j$  factor as rescaling coefficients of the Hamiltonian and keep each step at  $T/5$ . Our results will not depend on this choice.

The topological response of the AFAI is most robustly found by considering a cylinder geometry in which the bottom half of the cylinder is initially filled and the top half is initially empty. Chiral edge states appear at the top and bottom edges, and our initial state ensures that only one edge state is filled. This edge state carries current around the cylinder at a quantized rate, while the bulk is localized and thus insulating. Hence, we have quantization of the total charge pumped per Floquet cycle ( $Q$ ), which is defined for a given Floquet cycle by

$$Q = \int_{t_0}^{t_0 + \tilde{T}} dt \langle \psi(t) | I_x | \psi(t) \rangle, \quad (6)$$

where  $I_x$  is the current operator in the  $x$  direction,  $\tilde{T} = \sum_\ell T_\ell$  is the Floquet period modified by the temporal noise, and  $t_0$  is the start of the Floquet cycle. Our parameters are chosen such that  $Q = 1$  in the topological phase. We simulate the system identically to the case with white noise; details may be found in Ref. [27].

*Results.* *A priori*, the effect of quasiperiodic temporal disorder on pumped charge ( $Q$ ) is not obvious. On one hand, quasiperiodically driven systems are amenable to localization, allowing the possibility of exponentially long-lived topological pumping. On the other hand, systems subjected to white noise display quantized topological response up to the Thouless time for sufficiently weak disorder, which was argued to result from direct averaging over multiple Floquet cycles [27]. By contrast, quasiperiodically driven systems do not self-average in this way, and in particular have the potential to give constructive interference of the pumping over multiple cycles that could destroy its quantization.

Therefore, we start with direct simulations of the charge pumped,  $Q(t)$ , as a function of system size, disorder, and noise strength. A characteristic trace is shown in Fig. 2 for  $W_x = 1$  and  $W_t = 0.1$ , which lies in the topological phase of the noisy model [27]. Both the white noise and quasiperiodic case show the same general trend—a short-time transient, followed by a long-lived quantized plateau, and finally decay towards  $Q = 0$ . We first note that charge pumping in the quasiperiodic case

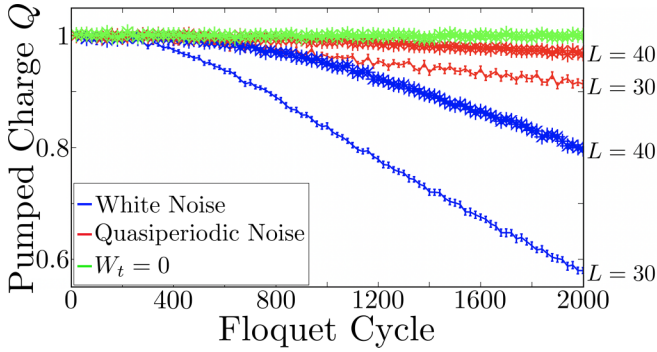


FIG. 2. Finite-size dependence of charge pumping ( $Q$ ) as a function of time with  $W_x = 1$ . White noise is seen to cause more rapid decay than quasiperiodic noise. The noisy curves have  $W_t = 0.1$ , well within the topological phase of the model with white noise [27].

decays much more gradually than the random noise case. This suggests that the topological phase is at least as stable in the quasiperiodic case as in the case of white noise. However, it still leaves open the possibility of a topological phase that extends to larger values of  $W_t$  and is, potentially, infinitely long-lived for some parameter values.

To better understand the topological behavior with quasiperiodic disorder, we study the behavior of decay time  $\tau$  as a function of system size  $L$ . A conventional topological plateau would survive to time  $\tau \sim \exp(L/\xi)$  for localization length  $\xi$ , but we do not see such exponential growth for any of the parameters simulated. This suggests that, for our parameter window, no stable topological phase exists with both real-space and frequency-space localization (cf. Ref. [29]). In the absence of such “conventional” multifrequency Floquet topology, an additional importance is placed on the longevity of the plateau region, since this determines the nature of our long-lived topological pumping. Therefore, we will proceed to study the dynamics of  $Q(t)$  to understand this stability more precisely. Similar to the noisy results, we will confirm that no absolutely stable region exists, but whereas white noise inevitably leads to diffusion, quasiperiodic drive can lead to subdiffusion. Towards this end, we postulate power-law scaling of the decay time,  $\tau \sim L^\alpha$ , and attempt to numerically find the value of  $\alpha$  as a function of spatial ( $W_x$ ) and temporal ( $W_t$ ) disorder.

While quantized charge pumping is the observable consequence of topology, it has strong finite-size effects that make it less useful for detecting topological phase transitions [17,27]. Instead, we use metrics for single-particle (Anderson) localization as sensitive detectors of the spatial and temporal dynamics of the wave function.

One conventional metric for localization is the level spacing ratio [36]. However, that requires identification of eigenstates, which are not easily accessible in our bichromatically driven system. Instead, we consider the participation ratio ( $P$ ), which is defined for an arbitrary single-particle state  $|\psi\rangle$  and position basis  $|\mathbf{r}\rangle$  as

$$P = \left( \sum_{\mathbf{r}} |\langle \mathbf{r} | \psi \rangle|^4 \right)^{-1}. \quad (7)$$

For a wave function that is fully delocalized in the position basis, such that each basis element occurs with probability  $p = 1/N_{\text{sites}}$ , the  $P$  is equal to the total number of sites,  $N_{\text{sites}} = L^2/2$ . By contrast, if the particle is localized on a single  $\mathbf{r}$  site, then  $P = 1$ . In general, for a  $d$ -dimensional system, we can think of  $P^{1/d}$  as a proxy for the localization length.

Here we consider the participation ratio for the wave function  $|\psi(NT)\rangle$  obtained by time-evolving an initial state  $|\psi(0)\rangle = |\mathbf{r} = (0, 0)\rangle$  located in the middle of the system for  $N \gg 1$  Floquet cycles. Participation ratios for various system sizes and noise strengths are shown in Fig. 3. The first thing we notice is that  $P$  is much smaller for quasiperiodic noise than for white noise, suggesting that, for a given time  $NT$ , the quasiperiodic system is much less delocalized than the white-noise case, which is known to delocalize diffusively. While a peak appears at finite  $W$ , this is not a direct sign of a phase transition, unlike the Floquet case, because the peak does not sharpen as a function of system size (data not shown). Instead, we notice strong finite-size effects and, more strikingly, large dependence on the evolution time  $NT$ . Empirically, we see that at large  $L$ —where finite-size effects can be neglected—the  $P$  appears to approach a power law scaling, with  $P \sim N^{0.70}$  for  $W_x = 1.5$  and  $W_t = 0.1$ . This is our first hint of subdiffusive dynamics, which we now probe in more detail.

Unlike conventional localization problems, this quasiperiodically driven system also has another axis in which localization must be probed. If we consider mapping the two-frequency Floquet problem to a photon lattice—the so-called Floquet extended zone picture—then the photons themselves live on a two-dimensional square lattice with energy tilt (“electric field”) proportional to the drive frequencies. This extended zone lattice is illustrated in Fig. 4(a). While Wannier-Stark localization along the electric field direction is guaranteed, localization in the orthogonal direction (green shaded area) depends on the precise model. In the language of Anderson localization, this orthogonal direction looks similar to quasiperiodic chemical-potential disorder via a cut-and-project method [37]. Taken together, the two spatial dimensions and two frequency dimensions give a single-particle localization problem in a quasi-three-dimensional space, with a combination of uncorrelated (real-space) and quasiperiodic (frequency-space) disorder. We are not aware of a solution to this localization problem. Furthermore, frequency-space localization has been shown to be fundamental in defining topological invariants for other quasiperiodically driven systems [28,29]. Therefore, frequency space localization will be required for exponentially long-lived topology in our model as well.

We study frequency-space localization via a generalized participation ratio, introduced in Ref. [29]. We start with a discrete Fourier transform of the time-evolved wave function:

$$|\psi_N(\omega)\rangle = N^{-1/2} \sum_{j=1}^N e^{ij\omega T} |\psi(jT)\rangle, \quad (8)$$

where  $\omega = 2\pi k/(NT)$  with  $k = 0, 1, \dots, N-1$ . If we think of this frequency space lattice as our basis, then the density

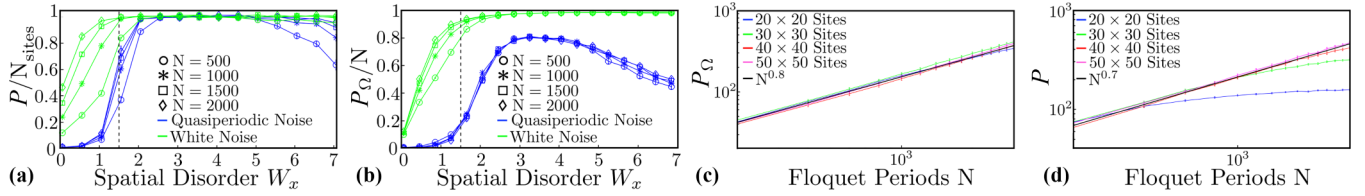


FIG. 3. Participation ratio ( $P$ ) in (a), (d) real space and (b), (c) frequency space with temporal disorder  $W_t = 0.1$ . (a), (b) Comparison of white noise and quasiperiodic drive as a function of number of Floquet periods for a system size of  $L = 30$  ( $N_{\text{sites}} = L^2/2$ ) in both (a) position space and (b) frequency space. Note that quasiperiodic drive consistently has smaller  $P_\Omega$ , indicating slower delocalization. (c) Time-dependence of frequency-space  $P$  and (d) spatial  $P$ , showing consistency with subdiffusion in real space and superdiffusive but sub-ballistic spreading in frequency space. In panels (c) and (d), the spatial disorder strength is  $W_x = 1.5$  as indicated by the dashed black line in panels (a) and (b).

for “site”  $\omega$  is given by

$$\rho_N(\omega) \propto \langle \psi_N(\omega) | \psi_N(\omega) \rangle. \quad (9)$$

We choose the normalization  $\sum_\omega \rho_N(\omega) = 1$  to match the conventional  $P$ . The frequency space  $P$  is then, by analogy,

$$P_\Omega = \left( \sum_\omega \rho_N(\omega)^2 \right)^{-1}. \quad (10)$$

As with real-space participation ratio,  $P_\Omega = N$  for the fully delocalized state and  $P_\Omega = 1$  for the fully localized state.

The frequency-space  $P$  is shown in Figs. 3(b) and 3(c). Similar to real-space  $P$ , it shows evidence of delocalization, with strong finite-size and finite-time dependence. A power-law fit gives  $P_\Omega \sim N^{0.8}$  for the parameters shown, which we analyze further below.

*Subdiffusion.* If we consider  $P^{1/2}$  and  $P_\Omega$  as proxies for the real- and frequency-space localization lengths, then the power-law fits in Fig. 3 are suggestive of subdiffusive motion. For  $W_x = 1.5$  and  $W_t = 0.1$ , Fig. 3(c) shows spatial  $P \sim r^2 \sim t^{0.70}$ , which is below  $r^2 \sim t$  that characterizes diffusion. Frequency-space  $P$  is more complicated, showing  $P_\Omega \sim t^{0.8}$ . Since frequency space is effectively one-dimensional due to Wannier-Stark localization along  $\tilde{\Omega}$ , this is superdiffusive but sub-ballistic. Most notably, frequency space and real space do not have the same exponents, indicating that particle delocalization is anisotropic in this extended zone picture.

We can study spatial subdiffusion directly by looking at the variance of the position in the time-evolved state,

$$R^2 = \langle \psi(NT) | r^2 | \psi(NT) \rangle. \quad (11)$$

Fitting this for a given value of spatial and temporal disorder, as illustrated in Fig. 4(b), we find clear subdiffusive power-law growth. A phase diagram of the subdiffusive exponent as a function of  $W_x$  and  $W_t$  is shown in Fig. 4(c). Note that the power laws obtained from  $R^2$  and those from  $P$  match within error bars [cf. Figs. 3(b) and 4(c)]. More importantly, the exponent shown here,  $R^2 \sim t^\alpha$ , matches that from the timescale for loss of quantized pumping,  $L^2 \sim \tau^\alpha$  as a loss of quantization, is caused by the depopulation of the edge states, which occurs on a timescale set by subdiffusion. Over the majority of the phase diagram, quasiperiodic drive shows clear differences from white noise, where the dynamics are always diffusive [27]. For sufficiently strong  $W_x$  and  $W_t$ , the dynamics is not readily distinguished from diffusion, which is consistent with the well-studied possibility of diffusion in three-dimensional disordered systems [38,39]. We have also added curves corresponding to the numerically identified topological phase transitions for the case with white noise, taken from Ref. [27]. Intriguingly, these transitions align somewhat closely with cases where the exponents appear to approach those of diffusion. One possible origin of this effect is the physics of the crossover phase, which was argued in Ref. [27] to occur for  $W_x \lesssim 3.6$  and  $W_t > W_{t,c}(W_x)$  (the phase to the right of the blue line in Fig. 4). In the crossover phase,

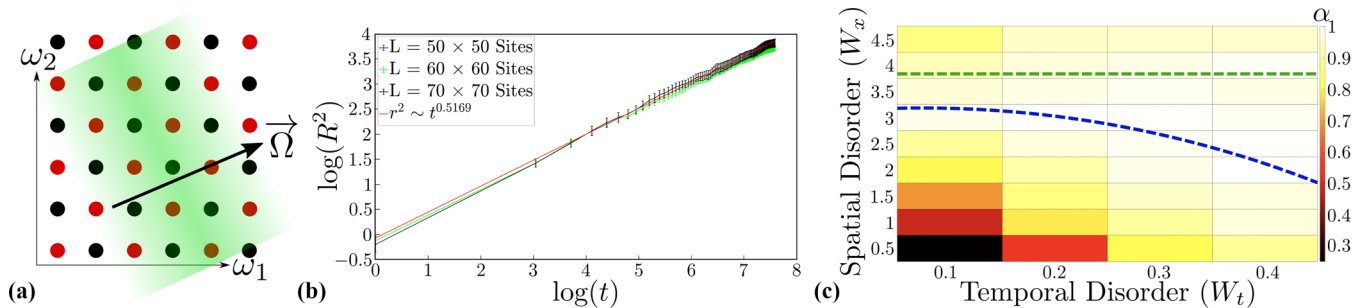


FIG. 4. (a) Illustration of the Floquet extended zone picture for two-mode driving. Frequencies  $\omega_1$  and  $\omega_2$  map to photons, whose wave function is Wannier-Stark localized in the direction parallel to the drive frequency ( $\tilde{\Omega}$ ). Localization perpendicular to  $\tilde{\Omega}$  (green shaded direction) depends on many factors, including irrationality of  $\omega_2/\omega_1$ . (b) Direct calculation of subdiffusion for  $W_x = 1$  and  $W_t = 0.1$ . The mean-square radius increases as  $\sim t^{0.5}$ , well below the diffusive exponent,  $t^1$ . (c) Dependence of subdiffusive exponent,  $R^2 \sim t^\alpha$ , on spatial and temporal disorder. Dashed lines show the phase boundaries for white noise, taken from Ref. [27].



some realizations of temporal noise correspond to a trivial Floquet problem, while others are topologically nontrivial. As the Anderson localized micromotion within these two phases is topologically incompatible, one may imagine that the cycles add “incoherently” despite the structured nature of the quasiperiodic drive. This would effectively restore true decohering noise, and could result in the observed diffusive spreading.

*Discussion.* We have seen topological pumping in a quasiperiodically driven variant of the anomalous Floquet-Anderson insulator (AFAI). Initially localized states spread subdiffusively, with exponents determined by the strength of spatial disorder ( $W_s$ ) and quasiperiodic temporal disorder ( $W_t$ ). In all situations, the quasiperiodically driven system is seen to be at least as stable as the equivalent noisy system. Given the existence of a stable topological phase with long-lived quantized pumping in the noisy system [27], our numerics suggest that such a stable topological phase exists in the quasiperiodically driven system as well; in particular, we predict that the topological phase diagram is identical to that in Ref. [27] (dashed lines in Fig. 4).

While it is encouraging that a topological phase persists at finite  $W_t$ , the nature of the phase and phase transitions remains unclear. It is not exponentially long-lived in system size, as is the case for conventional topological phases of matter that are Anderson localized; despite our best attempts, no fully localized points in the phase diagram were found. In general, the study of combined Wannier-Stark and Anderson localization in systems like ours remains an interesting unsolved problem. Yet we can hope that variants of the model may be found in which localization is present in both spatial and frequency directions, for which a topological invariant can be defined by analogy with the noiseless case. Given that the topological pumping only relates to the original Floquet cycle  $T = 2\pi/\omega_1$ , we expect any topological invariant to integrate over the  $\omega_2$  direction. Inspired by the three-dimensional Chern insulator [40,41], and more generally weak and/or higher-order topology [42–44], we therefore propose the following topological winding number to characterize the transient

quantized pumping  $Q^* = \nu$  with

$$\nu = \frac{1}{16\pi^3} \int d\theta_x d\theta_y d\phi_1 d\phi_2 \text{Tr}(P^\dagger \partial_{\phi_1} P [P^\dagger \partial_{\theta_x} P, P^\dagger \partial_{\theta_y} P]),$$

where  $\theta_x$  and  $\theta_y$  are the magnetic fluxes through the  $x$ ,  $y$  directions of the torus with periodic boundary conditions,  $\phi_1$  and  $\phi_2$  are the phase of the drives at frequencies  $\omega_1$  and  $\omega_2$ , and  $P(\vec{\theta}, \vec{\phi})$  is the generalized micromotion operator [29]. In the absence of disorder, this object is well defined and quantized as long as the generalized Floquet eigenstates are localized in photon space. In the presence of disorder, it is only clearly defined for finite systems, but may lose quantization as we take  $L \rightarrow \infty$  due to delocalization. A similar loss of quantization occurs in the nontopological “crossover” regime at large  $W_t$ , for which we expect that  $\nu$  is no longer independent of  $\phi_2$ . A more explicit connection between this proposed topological invariant and measurable responses such as edge-state charge pumping ( $Q$ ) will be a topic for future research.

Finally, we note that, were the problem localized in both frequency and position space, it would admit an alternative four-dimensional topological description. There are fewer obvious candidates for (non-symmetry-protected) topology in four dimensions, as the winding numbers usually used for Floquet topology are only defined in odd dimensions [44,45]. One possibility is to look for a nontrivial second Chern number [46,47]. Whether second Chern insulators can be extended to a bichromatically driven two-dimensional system is an interesting open question.

*Acknowledgments.* We thank Sarang Gopalakrishnan and Lukas Sieberer for valuable discussions. This work was performed with support from the National Science Foundation through Grant No. DMR-1945529 and the Welch Foundation through Grant No. AT-2036-20200401. We used the computational resources of the Lonestar 5 cluster operated by the Texas Advanced Computing Center at the University of Texas at Austin and the Ganymede and Topo clusters operated by the University of Texas at Dallas’ Cyberinfrastructure & Research Services Department.

- 
- [1] P. Cejnar, P. Stránský, M. Kloc, and M. Macek, *AIP Conf. Proc.* **2150**, 020017 (2019).
- [2] V. Khemani, A. Lazarides, R. Moessner, and S. L. Sondhi, *Phys. Rev. Lett.* **116**, 250401 (2016).
- [3] C. W. von Keyserlingk and S. L. Sondhi, *Phys. Rev. B* **93**, 245146 (2016).
- [4] D. V. Else, B. Bauer, and C. Nayak, *Phys. Rev. Lett.* **117**, 090402 (2016).
- [5] S. Choi, J. Choi, R. Landig, G. Kucsko, H. Zhou, J. Isoya, F. Jelezko, S. Onoda, H. Sumiya, V. Khemani *et al.*, *Nature (London)* **543**, 221 (2017).
- [6] J. Zhang, P. W. Hess, A. Kyprianidis, P. Becker, A. Lee, J. Smith, G. Pagano, I.-D. Potirniche, A. C. Potter, A. Vishwanath *et al.*, *Nature (London)* **543**, 217 (2017).
- [7] D. V. Else, C. Monroe, C. Nayak, and N. Y. Yao, *Annu. Rev. Condens. Matter Phys.* **11**, 467 (2020).
- [8] V. Khemani, R. Moessner, and S. L. Sondhi, [arXiv:1910.10745](https://arxiv.org/abs/1910.10745).
- [9] X. Mi, M. Ippoliti, C. Quintana, A. Greene, Z. Chen, J. Gross, F. Arute, K. Arya, J. Atalaya, R. Babbush, J. C. Bardin, J. Basso, A. Bengtsson, A. Bilmes, A. Bourassa, L. Brill, M. Broughton, B. B. Buckley, D. A. Buell, B. Burkett *et al.*, *Nature (London)* **601**, 531 (2022).
- [10] M. S. Rudner, N. H. Lindner, E. Berg, and M. Levin, *Phys. Rev. X* **3**, 031005 (2013).
- [11] R. Roy and F. Harper, *Phys. Rev. B* **94**, 125105 (2016).
- [12] C. W. von Keyserlingk and S. L. Sondhi, *Phys. Rev. B* **93**, 245145 (2016).
- [13] D. V. Else and C. Nayak, *Phys. Rev. B* **93**, 201103(R) (2016).
- [14] A. C. Potter, T. Morimoto, and A. Vishwanath, *Phys. Rev. X* **6**, 041001 (2016).
- [15] F. Nathan and M. S. Rudner, *New J. Phys.* **17**, 125014 (2015).
- [16] R. Roy and F. Harper, *Phys. Rev. B* **96**, 155118 (2017).
- [17] P. Titum, E. Berg, M. S. Rudner, G. Refael, and N. H. Lindner, *Phys. Rev. X* **6**, 021013 (2016).

- [18] H. C. Po, L. Fidkowski, T. Morimoto, A. C. Potter, and A. Vishwanath, *Phys. Rev. X* **6**, 041070 (2016).
- [19] A. C. Potter and T. Morimoto, *Phys. Rev. B* **95**, 155126 (2017).
- [20] F. Harper and R. Roy, *Phys. Rev. Lett.* **118**, 115301 (2017).
- [21] R. Roy and F. Harper, *Phys. Rev. B* **95**, 195128 (2017).
- [22] H. C. Po, L. Fidkowski, A. Vishwanath, and A. C. Potter, *Phys. Rev. B* **96**, 245116 (2017).
- [23] A. C. Potter, A. Vishwanath, and L. Fidkowski, *Phys. Rev. B* **97**, 245106 (2018).
- [24] D. Reiss, F. Harper, and R. Roy, *Phys. Rev. B* **98**, 045127 (2018).
- [25] M. H. Kolodrubetz, F. Nathan, S. Gazit, T. Morimoto, and J. E. Moore, *Phys. Rev. Lett.* **120**, 150601 (2018).
- [26] F. Nathan, D. Abanin, E. Berg, N. H. Lindner, and M. S. Rudner, *Phys. Rev. B* **99**, 195133 (2019).
- [27] C. I. Timms, L. M. Sieberer, and M. H. Kolodrubetz, *Phys. Rev. Lett.* **127**, 270601 (2021).
- [28] D. M. Long, P. J. D. Crowley, and A. Chandran, *Phys. Rev. Lett.* **126**, 106805 (2021).
- [29] F. Nathan, R. Ge, S. Gazit, M. Rudner, and M. Kolodrubetz, *Phys. Rev. Lett.* **127**, 166804 (2021).
- [30] C. L. Kane and E. J. Mele, *Phys. Rev. Lett.* **95**, 226801 (2005).
- [31] L. Fu, C. L. Kane, and E. J. Mele, *Phys. Rev. Lett.* **98**, 106803 (2007).
- [32] D. V. Else, W. W. Ho, and P. T. Dumitrescu, *Phys. Rev. X* **10**, 021032 (2020).
- [33] P. T. Dumitrescu, R. Vasseur, and A. C. Potter, *Phys. Rev. Lett.* **120**, 070602 (2018).
- [34] A. J. Friedman, B. Ware, R. Vasseur, and A. C. Potter, *Phys. Rev. B* **105**, 115117 (2022).
- [35] S. Iyer, V. Oganesyan, G. Refael, and D. A. Huse, *Phys. Rev. B* **87**, 134202 (2013).
- [36] V. Oganesyan and D. A. Huse, *Phys. Rev. B* **75**, 155111 (2007).
- [37] K. Singh, K. Saha, S. A. Parameswaran, and D. M. Weld, *Phys. Rev. A* **92**, 063426 (2015).
- [38] A. Legendijk, B. van Tiggelen, and D. S. Wiersma, *Phys. Today* **62**(8), 24 (2009).
- [39] P. W. Anderson, *Phys. Rev.* **109**, 1492 (1958).
- [40] S. Liu, T. Ohtsuki, and R. Shindou, *Phys. Rev. Lett.* **116**, 066401 (2016).
- [41] M. Kolodrubetz, *Phys. Rev. Lett.* **117**, 015301 (2016).
- [42] A. Dutt, M. Minkov, I. A. D. Williamson, and S. Fan, *Light: Sci. Appl.* **9**, 131 (2020).
- [43] Y. Xue, H. Huan, B. Zhao, Y. Luo, Z. Zhang, and Z. Yang, *Phys. Rev. Res.* **3**, L042044 (2021).
- [44] F. Nathan, M. S. Rudner, N. H. Lindner, E. Berg, and G. Refael, *Phys. Rev. Lett.* **119**, 186801 (2017).
- [45] F. N. Únal, B. Seradjeh, and A. Eckardt, *Phys. Rev. Lett.* **122**, 253601 (2019).
- [46] L. Zhou, Y. Gu, and J. Gong, *Phys. Rev. B* **103**, L041404 (2021).
- [47] H. Wu, B.-Q. Wang, and J.-H. An, *Phys. Rev. B* **103**, L041115 (2021).